International Conference on Recent Trends in Materials and Characterization (RETMAC -2010)
February 14 – 15, 2010, National Institute of Technology, Suratkal, Karnataka.

# Electrochemical Synthesis Of Cu Thin Films Under Ultrasonic Irradiation: The Effect On Ex-situ Growth Behavior

S. Rout*, A. Mallik and B. C. Ray
*Department of Metallurgical and Materials Engg.*
*National Instityute of Technology,*
*Rourkela, 769008*
*India*
**sabita.swain1@gmail.com*

**Abstract:**

The nucleation and growth phenomena taking place under the impact of intense ultrasonic field during deposition of copper films onto graphite substrate from sulphate bath has been investigated. A comparative study of crystallinity, composition and ex-situ growth behavior of the as-deposited copper thin films and similar films prepared under ultrasonic irradiation are carried out. The thermodynamics and kinetics of the growth behaviour studied, utilizing calorimetric techniques.

**Keywords:** Copper, Electrodeposition, Thin-film, Ultrasound, Growth

## 1. Introduction:

The electrocrystallization of copper on foreign substrates is a matter of great technological interest. The process has been widely used in electronic industry for interconnects, manufacturing of printed circuit boards and multilayer sandwitches of GMR hard disc read heads. It is also used as commercial catalysts in fuel cells and in hydrogenation process[1-3]. The graphite substrate is a suitable support for a wide variety of metal catalyst due to its high electrical and mechanical properties, a high thermal stability and a low cost[4]. The metallic films of adequate thickness, structure and adhesion could be achieved through electrodeposition by altering its electrochemical parameters such as concentration of electrolyte, $P^H$ of bath solution, types of bath, temperature, types of substrate, deposition potential[4-11]. Moreover the imposition of high intensity ultrasound with the conventional electrodeposition imparts increased deposition hardness, improved deposition rates and efficiencies and greater adhesion of the deposit to the electrode. These effects are attributed to acoustic streaming increasing mass transport to the electrode surface, resulting from the appearance and collapse of cavitational bubbles and ultrasonic degassing of solutions[12,13,14].

The growth of the electrodeposited film in real applications is of great concern which leads to the impairment of the properties of the thin film. So the study of the kinetics and thermodynamics of the growth behavior is essential. Growth takes place by the atomic motion along the grain boundaries, free surfaces, dislocations. The energy density of the grain boundaries is the driving force for the grain growth. The energy density initially present in the as-deposited grain boundaries is lowered by the process of grain growth. Growth can be normal or abnormal depending upon the driving force. The normal grain growth follows the parabolic law[15] as in (Eqn. (1))

$$D = D_0^2 + kt \qquad (1)$$

Where D and $D_0$ are the mean grain diameter of the films after and before growth and t is the time of a thermal treatment. The presence of grains with diameters exceeding ten times the film thickness signifies abnormal or secondary grain growth. It may occur when there is an additional driving force for grains to grow beyond the usual limit of normal grain growth or when the normal grain growth is hindered by a particle pinning mechanism. This type of growth is rapid and abrupt which can only be explained in terms of a significant increase of grain boundary mobility. Moreover the growth of the grains due to their different sizes can be elucidated by the mechanism of Ostwald ripening process in which the larger particles grow at the expense of smaller ones. The smaller particles are more soluble than larger ones. Thus smaller particles tend to lose their molecules and these molecules diffuse through the continuous phase and re-precipitate onto larger particles. This leads to an increase of average particle size[16]. The growth of the film also takes place by the presence of triple junction grain boundaries in which for the establishment of equilibrium angle of 120° between the grain boundaries, gradually engulfs the grain boundaries of smaller or larger deviation values. To control the grain growth, Zener pinning effect and grain boundary grooving are two established mechanism[17].

In this paper, the electrodeposition of copper on the graphite substrate from aqueous solution of copper sulphate at various over-potentials under the effect of ultrasonic irradiation is discussed. As the cathodic potential increases, the size of the copper grains are predicted to decrease with densified grain distribution. But by the application of high intense ultrasonic field the densified grain distribution with high agglomerates are predicated to achieve at lower deposition potential. The present paper will explore it by comparison of the chronoamperometric current transients (CCT) and SEM micrographs of the samples at various over-potentials both at silent and sonication. Analysis of the behavior in the absence and presence of the ultrasonic irradiation are carried out by X-Ray diffraction (XRD) and Atomic force Microscopy (AFM). The study of thermodynamics and rate kinetics of the film growth are performed by differential scanning calorimeter (DSC).

## 2. Experimental:

Analytical grade $CuSO_4.5H_2O$ (10 $gl^{-1}$) and $H_2SO_4$(40 $gl^{-1}$) have been for the preparation electrolytes for copper deposition. The solution is prepared with doubly distilled water. Copper is electrochemically deposited on the graphite substrate of an exposed surface area of 0.25 $cm^2$. Prior to each experiment, the plates are polished to mirror finish and then cleaned in an ultrasonic cleaner (20 kHz frequency) for 10 minutes. The Electrochemical experiments were performed with a potentiostat/galvanostat (Eco Chemic Netherland, Autolab PGSTAT 12) system having computer interface of GPES software. A standard three-electrode cell is assembled. A Pt rod of 3.5 $cm^2$ surface area is used as counter electrode, and an Ag/AgCl reference electrode is used. Morphological studies of prepared samples are performed by means of SEM (JEOL 6480LV) and AFM (Veeco diInnova). The phase analysis is done with XRD (Philips x-pert MPD), and the patterns are recorded from 40-100° at a scanning rate of 1°/Min with CuKα radiation. The growth analysis is carried out using DSC (Mettler Toledo-DSC822$^e$). Experiment is performed at a temperature range of 25 – 400 °C at a rate of 2 °/min.

## 3. Results and Discussions:

The chronoamperometric curves of Cu electrodeposition on the graphite electrode prepared in silent and sonication conditions are illustrated in figure 1. The transient plots in silent condition show an initial increase in the cathodic current density followed by a gradual decrease over time. The reduction reactions on the electrode producing nuclei occur instantly, resulting in a high current density. These reduction reactions consume the reducing ionic species at the surface of the electrode and create a depletion zone where the concentrations of the ionic species are low at the electrode surface but are progressively higher away from the surface. The diminishing concentrations of the reducing ionic species in the depletion zone cause the current density to drop continuously. When diffusion of the reducing ionic species from the bulk solution to the depletion region is just sufficient to permit continuous reduction, the current density reach a constant value. A constant current density indicates a diffusion-controlled process. The shape of the insonicated current transient as shown in fig1(b) is significantly altered compared to that of silent counterpart. A slow current decay under silent condition is replaced under insonicated condition by a sharp decay that is followed by a series of crests and troughs depicting secondary nucleation due to crystal breakage [18]. The measured kinetic parameters of the current transients of the copper deposits are shown in table1. The calculated thickness [18] of the films varies from 120 nm to 1.1 μm.

The XRD patterns of the samples synthesized at different overpotentials are as shown in figure 2. Decrease in either domain size or lattice strain will cause effective broadening of diffracted peaks. The peak pattern shows high crystallinity of copper along with peaks from the substrate material. The diffraction peaks at 2θ = 43.317, 50.449, 74.126, 89.938 can be indexed as the (111), (200) , (220), (311) planes of copper with cubic symmetry respectively (JCPDS card no: 85-1326).

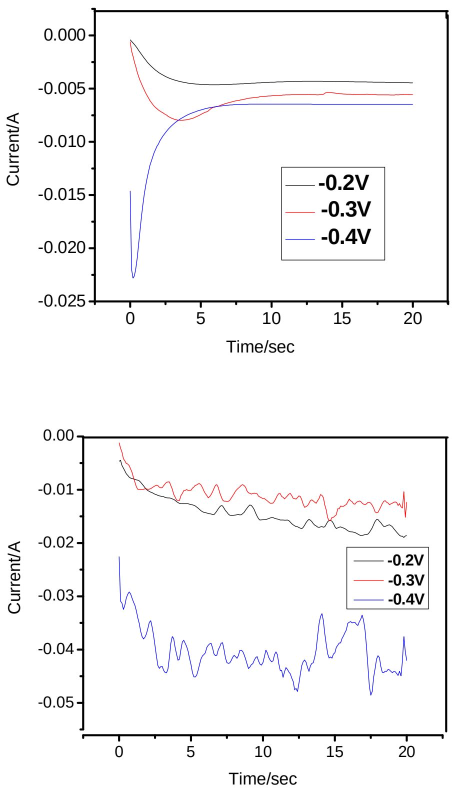


**Fig.1: Chronoamperometry of Copper deposition at (a) silent and (b) sonication conditions**

Average crystallite sizes of copper deposit were determined by the Williamson-Hall formula (As Scherrer equation is valid only for powders or loosely bound deposits but not for hard and adherent deposits). Average crystallite size of copper deposit varies from 74 to 6 nm with strain level variation of 0.0005 to 0.01.

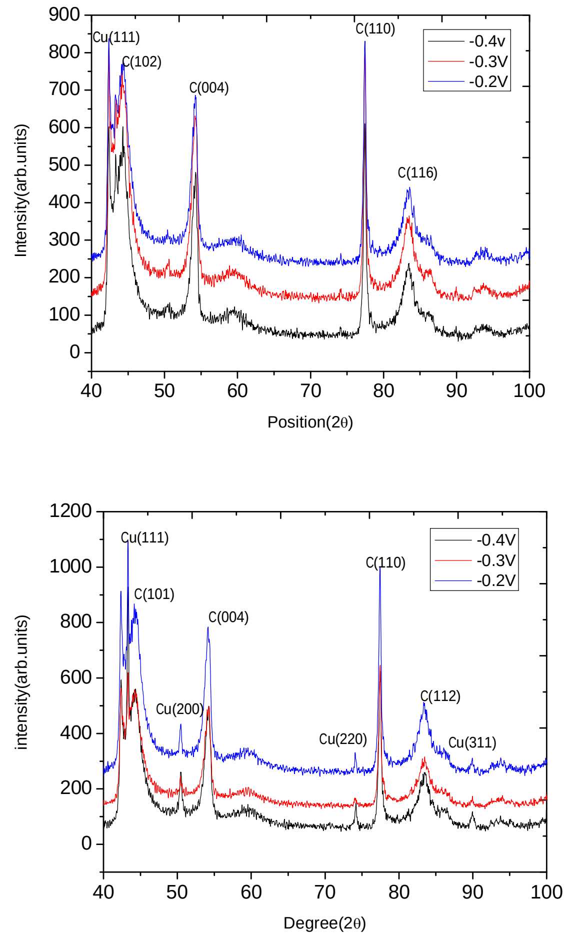


**Figure 2: XRD plots of Cu deposition for (a) Silent and (b) Sonication conditions**

**Table 1: Characteristic kinetics parameters of i(t) transients obtained for copper deposits obtained for different deposition potentials**

| $E_{dep}$(V) | $I_{max}$(A/cm$^2$) | | $t_{max}$(sec) | | D x10$^{-16}$(cm$^2$s$^{-1}$) | | $N_0$ x10$^{11}$ (cm$^{-2}$) | | $Q_{total}$(C) | |
|---|---|---|---|---|---|---|---|---|---|---|
| | **Silent** | **US** | **Silent** | **US** | **Silent** | **US** | **Silent** | **US** | **Silent** | **US** |

| | | | | | | | | | | |
|---|---|---|---|---|---|---|---|---|---|---|
| **-0.2** | **-0.00462** | **-0.0147** | **5.4** | **6.57** | **1.8995** | **23** | **2.18** | **.14** | **-0.0831** | **-0.288** |
| **-0.3** | **-0.00797** | **-0.01** | **3.7** | **1.64** | **3.8733** | **2.7** | **1.56** | **5** | **-0.119** | **-0.229** |
| **-0.4** | **-0.0227** | **-0.0323** | **0.2** | **0.295** | **1.6984** | **5.0721** | **65** | **15** | **-0.153** | **-0.801** |

Figure 3 shows the SEM topographies of copper deposits both in static and sonication condition at different potentials. In static condition the grains formed decreases in size with increasing overpotential. In addition to this the surface coverage of copper nuclei also varies with the overpotential. The deposited copper nuclei bear the spherical shape with non uniform distribution. But under the effect of intense ultrasonic irradiation the topography is different. Nano-sized agglomerated spheroids of copper are formed with better surface coverage as compared to that deposited in silent condition. The high degree of aggregation had lead to a firm and adherent morphology. This can be elucidated by the fact that, in the presence of ultrasound the crystal fragmentation has nucleated a large number of copper grains. Copper is a highly reactive metal and is having always tendency towards agglomeration. Along with the enhancement in the mass transport due to cavitation, it also generates shock waves during the formation and collapse cycle. And the generated shock wave may further assist the agglomeration mechanism. The rate of agglomeration can further be analyzed from AFM studies (Fig. 4). The extent of agglomeration is clearly visualized from the micrographs. Higher the deposition potential higher is the agglomeration. Because of the grain distribution, habitat, film continuity and adherence the deposition at −0.4 V was selected for growth studies. Figure 5 shows the DSC scans of the deposits. Prominent peaks attributed to the growth phenomena are visible. It can be observed that the growth of the single phase silent copper has started from the start of the analysis temperature. And the amount of heat evolved is 0.14 W and 0.4 W for the static and sonication conditions respectively. This behavior may be the release of high residual stresses associated with the film during the deposition. On the other hand the sonicated deposit has less in-situ stress, as shown from the near parallel plateau of the analysis. The heat evolved for the insonicated film has a sharp peak in comparison to the shallow one for static condition. The discontinuities in the temperature vs. heat evolved plot for sonicated film may be due to the layer by layer growth evolution and melting of the film. The abrupt decrease in the melting of the film from 1083 °C to 400 °C is unambiguous for the nano-structured deposition. The depositions are further analyzed by SEM to support the thermal analysis. Figure 5 shows the after DSC scanned SEM micrographs. Static deposition grains have grown from 1 μm to 5 μm agglomerates. The deposition under sonication has grown abruptly and the surface coverage has decreased from the as deposited film. This may be due to the melting of the nano grains.

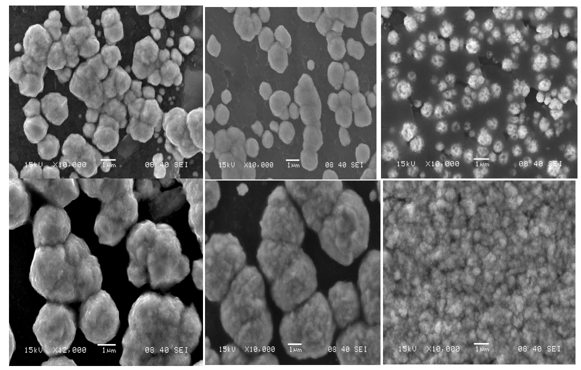

**−0.2V** **−0.3V** **−0.4V**

**Figure 3: SEM images of Cu deposits for (a-c) Silent and (d-f) Sonication conditions**

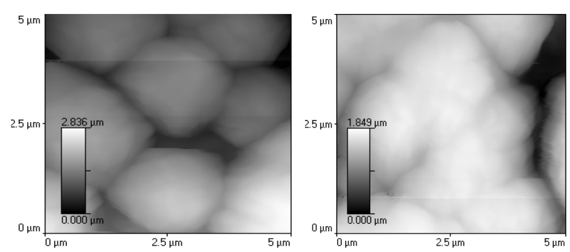


**Figure 4: AFM images of sonicated Cu deposits at (a) −0.3V and (b) −0.4V**

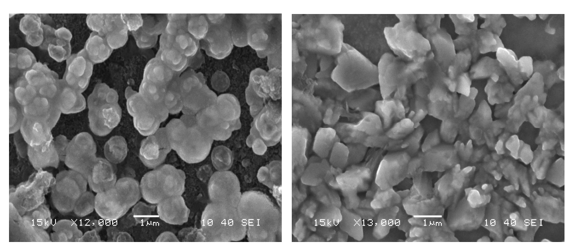

**Figure 5: SEM images of Cu deposits at −0.4V after DSC (a) silent and (b) sonication**

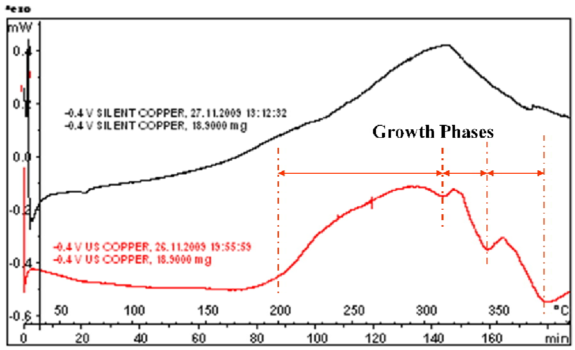


**Fig. 6: DSC plots for Cu thin films deposited at −0.4 V**

## 4.Conclusion:

Chronoamperometry, SEM and AFM studies have been carried out for Cu electrodeposition from $CuSO_4$(10 $gl^{-1}$), $H_2SO_4$(40 $gl^{-1}$) onto graphite under ultrasonic irradiation at various overpotentials. Depositions under silent conditions have the conventional tendency of decreased nuclei size and hence increased population density with elevated deposition potentials. Agglomerated grains with firm adherent morphology, good surface coverage and grain habitat has been observed under ultrasonic irradiation. The growth studies show highly stressed deposition for static condition, whereas sonicated films are dense and less stressed. The morphologies of the films are also distinguished after the growth phase. The exploration of the growth properties may significantly contribute to reemerge the sonoelectrochemistry field.

## Acknowledgement


The authors thank the National Institute of Technology (NIT),Rourkela for providing the necessary financial and infrastructural support.


## References:


1. Z.Grubac, M.Metikos-Hukovic, " *Nucleation of copper on an assembly of carbon microelectrodes*" Materials letters. **61**, 794(2007).

2. Anette A. Rasmussen, Jens A.D. Jensen, Andy Horsewell, Marcel A.J. Somers, "*Microstructure in electrodeposited copper layers: the role of the substrate*" Electrochimica Acta. **47**, 67(2001).

3. Wei Li, Chong Han, Wei Liu, Minghui Zhang, Keyi Tao, "*Expanded graphite applied in the catalytic process as a catalyst support*" Catalysis Today. **125**, 278(2007).

4. Ouassim Ghodbane, Lionel Roue, Daniel Belanger, "*Copper electrodeposition on pyrolytic graphite electrodes: Effect of the Cu salt on the eletrodeposition process"* Electrochimica Acta. **52**, 5843(2007).

5. Cheng-min Shen, Xiao-gang Zhang, Hu-lin Li, "*Effect of pH on the electrochemical deposition of cadmium selenide nanocrystal films*" Materials science and engineering. **B84**, 265(2001).

6. Zulkarnain Zainel, Anuar Kassim, Mohd Zobir Hussein, Chuah Hang Ching, "*Effect of bath temperature on the electrodeposition of copper tin selenide films from aquous solution*" Material Letters. **58**, 2199(2004).

7. S.M.S.I. Dulal, Hyeong Jin Yun, Chee Burm Shin, Chang-Koo Kim, " *Electrodeposition of CoWP film. Effect of pH and temperature*" Electrochimica Acta. **53**, 934(2007).

8. Neboji D. Nikolic, Goran Brankovic, Vesna M. Maksimovic, Miomir G.Pavlovic, Konstantin I.Popov, "*Influence of potential pulse conditions on the formation of honeycomb-like copper electrodes*" Journal of Electroanalytical chemistry. **635**, 111(2009).

9. Alejandro Martinez-Ruiz, Manuel Palomar-Pardave, Nikola Batina, "*Overpotential deposition of copper on an iodine-modified Au(111) electrode*" Electrochimica Acta. **53**, 2115(2008).

10. J.W.Faust, "*Effect of electrodeposition parameters on growth habit and morphology*" Journal of crystal growth. **3**, 433(1968).

11. Fereshteh Ebrahimi, Zunayed Ahmed, "*The effect of substrate on the microstructure and tensile properties of electrodeposited nanocrystalline nickel*" Materials Characterization. **49**, 373(2003).

12. Michael E.Hyde, Richard G. Compton, "*How ultrasound influences the electrodeposition of metals*" Journal of Electroanalytical Chemistry. **531**, 19(2002).

13. A.Mallik, B.C.Ray, "*Morphological study of electrodeposited copper under the influence of ultrasound and low temperature*" Thin Solid films. **517,** 6612(2009).

14. Hong Li, Hairong Li, Zhichao Guo, Yu Liu, "*The application of power ultrasound to reaction crystallization*" Ultrasonics sonochemistry. **13**, 359(2006).

15. P.R.Rios, "*Comparison between a computer simulated and an analytical grain size distribution*" Scripta Materialia. **40**, 665(1999).

16. Robert Finsy "*On the critical radius in Ostwald Ripening"* Langmuir. **20**, 2975(2004).

17. J.M.E. harper, C.Cabral, P.C.Andricacos, L.Gignac, I.C.Noyan, "*Mechanisms for microstructure evolution in electroplated copper thin films near room temperature*" Journal of applied physics. **86**, 2516(1999).

18. A. Mallik, A. Bankoti, B. C. Ray, "*A study on the modification of conventional electrochemical crystallization under sonication: The phenomena of secondary nucleation*" Electrochemical and Solid State Letters, **12** F46 (2009).